An Advanced Multifunctional Hydrogel-Based Dressing for Wound Monitoring and Drug Delivery

Bahram Mirani,
Center for Advanced Materials and Related Technologies (CAMTEC), University of Victoria, Victoria, BC V8P 5C2, Canada. Center for Biomedical Research, University of Victoria, Victoria, BC V8P 5C2, Canada. Laboratory for Innovations in Microengineering (LiME), Department of Mechanical Engineering, University of Victoria, Victoria, BC V8P 5C2, Canada

Erik Pagan,
Laboratory for Innovations in Microengineering (LiME), Department of Mechanical Engineering, University of Victoria, Victoria, BC V8P 5C2, Canada

Barbara Currie,
Department of Biochemistry and Microbiology, University of Victoria, Victoria, BC V8P 5C2, Canada

Mohammad Ali Siddiqui,
Laboratory for Innovations in Microengineering (LiME), Department of Mechanical Engineering, University of Victoria, Victoria, BC V8P 5C2, Canada

Reihaneh Hosseinzadeh,
Center for Advanced Materials and Related Technologies (CAMTEC), University of Victoria, Victoria, BC V8P 5C2, Canada. Center for Biomedical Research, University of Victoria, Victoria, BC V8P 5C2, Canada. Laboratory for Innovations in Microengineering (LiME), Department of Mechanical Engineering, University of Victoria, Victoria, BC V8P 5C2, Canada

Dr. Pooria Mostafalu,
Division of Engineering Medicine, Department of Medicine, Brigham and Women's Hospital, Harvard Medical School, Cambridge, MA 02139, USA

Dr. Yu Shrike Zhang,
Division of Engineering Medicine, Department of Medicine, Brigham and Women's Hospital, Harvard Medical School, Cambridge, MA 02139, USA

Prof. Aziz Ghahary, and
Division of Plastic Surgery, Department of Surgery, Faculty of Medicine, Vancouver, BC V5Z 1M9, Canada

Prof. Mohsen Akbari

Correspondence to: Mohsen Akbari.

Conflict of Interest
The authors declare no conflict of interest.

Center for Advanced Materials and Related Technologies (CAMTEC), University of Victoria, Victoria, BC V8P 5C2, Canada. Center for Biomedical Research, University of Victoria, Victoria, BC V8P 5C2, Canada. Laboratory for Innovations in Microengineering (LiME), Department of Mechanical Engineering, University of Victoria, Victoria, BC V8P 5C2, Canada

Abstract

Wound management is a major global challenge and poses a significant financial burden to the healthcare system due to the rapid growth of chronic diseases such as diabetes, obesity, and aging population. The ability to detect pathogenic infections and release drug at the wound site is of the utmost importance to expedient patient care. Herein, this study presents an advanced multifunctional dressing (GelDerm) capable of colorimetric measurement of pH, an indicator of bacterial infection, and release of antibiotic agents at the wound site. This study demonstrates the ability of GelDerm to detect bacterial infections using in vitro and ex vivo tests with accuracies comparable to the commercially available systems. Wireless interfaces to digital image capture hardware such as smartphones serve as a means for quantitation and enable the patient to record the wound condition at home and relay the information to the healthcare personnel for following treatment strategies. Additionally, the dressing is integrated within commercially available patches and can be placed on the wound without chemical or physical irritation. This study demonstrates the ability of GelDerm to eradicate bacteria by the sustained release of antibiotics. The proposed technology holds great promise in managing chronic and acute injuries caused by trauma, surgery, or diabetes.

Keywords

drug-delivery; infections; sensing; wound dressings; wound management

1. Introduction

Skin is the largest organ in the body, and it regulates body temperature, protects internal organs against external physical and chemical substances, and provides a physical barrier against pathogens and microorganisms.[1] Skin injuries caused by trauma, surgery, or diabetes have a high prevalence, and they represent a significant burden to patients and the healthcare system.[1] Skin damage is painful and can catastrophically compromise the integrity and protective functions of the skin and establish an active portal for infections. The latter is a major clinical challenge as wound infections result in significantly longer hospitalization, delayed wound healing, and increased cost and mortality.[2,3] Furthermore, an infection can lead to the development of a pronounced immune response, accompanied by sepsis or septic shock, which results in hypotension and multiorgan failure.[4] Therefore, prevention and management of infections, accompanied by continuous monitoring of the wound, are primary concerns of patients dealing with nonhealing or traumatic injuries.

Current treatment strategies aim to alleviate pain following trauma, protect the wound from pathogenic infections, maintain the moisture of the wound, manage exudates, and provide an environment that promotes the healing process. Depending on the extent of the injury, traditional dressings such as gauzes, cotton wools, dressings that deliver bioactive

constitutes, and antimicrobial and regenerative agents are being used in clinical practice. Commercially available dressings with regenerative capabilities include acellular grafts such as Alloderm (LifeCell), GraftJacket (KCI), Integra (Integra), and Biobrane (Smith & Nephew) as well as cellular grafts such as Dermagraft (Organogenesis), Epicel (Genzyme), and Recell (Avita). Silver-impregnated dressings are used extensively to prevent infections in the wound; some commercial examples are Acticoat (Smith & Nephew), Fibracol (Johnson & Johnson), and Silvasorb (Medline). However, there are several major challenges associated with implementing current dressings for wound management. First, it is almost impossible to detect pathogenic infections before clinical signs and symptoms arise. Second, the uncontrolled release of antimicrobial agents can lead to antibiotic resistance or delayed healing. Last, changing the dressing daily for visual inspections of the wound can be cumbersome and painful. Therefore, there is a pressing need to develop multifunctional dressings that are capable of monitoring wound conditions and providing proper treatment when necessary.

With the advent of flexible electronics and development of novel biomaterials, several advanced dressings have emerged that can measure the physicochemical properties of the acute and chronic wounds.[5–9] Kim et al. developed flexible electronic systems that possessed elasticity and bending stiffness that was similar to the epidermis.[5] These electronic devices were able to conform to the irregular structure of the skin and measure the temperature and strain on the skin. In another study, Huang et al. fabricated stretchable sensors that could be mounted on various elastomeric substrates including cellulose paper, polyurethane, and silicon for epidermal analysis of biofluids.[6] This device could quantify skin pH from sweat, then transfer data wirelessly to an external device. Najafabadi et al. fabricated electrical circuits on biodegradable nanofibrous polymeric substrates composed of a blend of poly(caprolactone) and poly(glycerol sebacate).[7] Temperature and strain sensors, as well as heating coils, were fabricated and characterized on this substrate. They demonstrated the ability to transfer the sensor readings and to control the heater wirelessly. Liu et al. developed flexible mechanoacoustic sensing electronics for epidermal measurement of cardiovascular diagnostics markers.[8] In a recent study, Mostafalu et al. developed a thread-based electronic system with the ability to measure physicochemical properties of tissues.[9] They used this technology to measure strain, temperature, pH, and glucose in biological samples. Despite being successfully implemented for epidermal applications, these electronic-based technologies face challenges that compromise their sensitivity because of the proteins, chemokines, and electrolytes which exist in wound exudates and sweat.[10] Moreover, electrical/electrochemical systems require the integration of electronic circuitry and a power source for analysis of their readout, complicating the device design and fabrication. These technologies have also not been combined with drug-releasing capabilities to deliver antimicrobial agents directly to the site of injury.

Colorimetric measurement of chemical biomarkers such as pH is an alternative approach that offers a simple quantitative method for continuous monitoring of the wound environment using devices such as smartphones that can capture high-quality digital images.[11] Herein, we report a multifunctional hydrogel-based dressing (GelDerm), capable of colorimetric measurement of pH as an indicator of bacterial infection and releasing antibiotics to wound site (Figure 1A). pH is an important indicator of the wound condition

and can be correlated to angiogenesis, protease activity, and bacterial infection.[12,13] The pH of the skin is slightly acidic and varies in the range of 4.0–6.0.[13] However, when the skin is breached in injuries, this acidic milieu is disturbed as the skin is exposed to internal body fluids that have a neutral pH (pH = 7.4).[13] GelDerm releases an antibiotic agent at the wound site continuously to sterilize the wound after the dressing is placed on the injury. The proposed engineered dressing offers several advantages over existing technologies including the ability to (1) map the pH of the wound using an array of printed sensors, (2) deliver antibacterial agents at the wound site, which prevents adverse side effects of systemic drug delivery, (3) maintain the wound moisture using a hydrogel substrate, and (4) provide conformal coverage to the wound area. Additionally, the dressing can be integrated within commercially available patches and can be placed on the wound without chemical or physical irritation.

2. Results

2.1. Multifunctional Hydrogel-Based Dressing (GelDerm) for Wound Monitoring and Drug Delivery

The multifunctional dressing introduced herein is composed of an array of porous, color-changing pH sensors and drug-eluting scaffolds, which were embedded within an alginate dressing (Figure 1A). The array of porous sensors (each sensor was 12 mm × 12 mm in size) was composed of 3D-printed color-changing alginate fibers that were loaded with mesoporous resin beads doped with a pH-responsive dye (Figure 1B). Alginate is a naturally derived polysaccharide that has been extensively used as a dressing material for epidermal applications due to its biocompatibility, hemostatic properties, and nonadhesive characteristics that facilitate the removal of the dressing without trauma and pain.[14–18] To print the sensors, a microextruder that consisted of two coaxial needles (Figure 1B; Figure S1, Supporting Information) mounted on a commercial 3D printer (Prusa i3) was used. The porosity of the sensors was adjusted by changing the diameter of the fibers while keeping the spacing between fibers constant. Encapsulation of the beads within the hydrogel fibers prevented the beads from dispersing in the wound area while providing a biocompatible interface with the wound site. Similarly, drug-eluting scaffolds were fabricated by 3D printing gentamicin-loaded alginate fibers (0.5–3.0 mg mL^{-1}). After fabrication, the dressing was first sterilized through exposure to ultraviolet (UV) light (365 nm, 200 mW cm^{-2}) and then lyophilized for storage and further usage. To obtain the optimum sterilization time, we intentionally contaminated the dressings with *Staphylococcus aureus* and *Pseudomonas aeruginosa* at the concentration of 10^5 colony-forming unit (CFU) and systematically increased the UV exposure times up to 30 min. Figure S2A (Supporting Information) shows the result of swab samples collected from UV-sterilized dressings that were grown on an agar plate. Our results indicated that a 30 min UV sterilization was adequate for eradicating bacterial contaminations in the dressings. Comparing UV-sterilized gentamicin with control (drug that was not treated with UV) showed no impact of the UV exposure on the antibacterial efficiency of the drug (Figure S2B,C, Supporting Information). Figure 1C shows a typical dressing after the lyophilization process. To improve the flexibility and mechanical integrity of the lyophilized dressings, we added glycerol, which is a well-known plasticizer for wound dressing and food packaging[19,20] to alginate (Figure

1C; Figure S3, Supporting Information). We used synthetic (Brilliant Yellow) and naturally derived (cabbage juice) pH indicators; however, other indicators can also be used in our system. The array of sensors enabled measuring the spatial variations of pH within the wound that could be caused by different bacterial infections (Figure 1D). The hydrogel dressings were flexible and could maintain a conformal contact with the irregular surface of the skin (Figure 1E).

2.2. Fabrication and Physical Characterization of GelDerm

3D printing using a microfluidic coaxial extruder, mounted on a programmable XYZ positioning stage, provided an efficient route to fabricate porous sensors. An important feature of the fabricated sensors, which could be controlled by the fiber diameter, was the available surface area per volume of the sensors. We hypothesized that more available surface per volume could significantly improve the response time of the sensors. Three bead densities of 3, 16, and 33% w/v were used to fabricate the sensors. Bead densities of more than 33% w/v were not printable due to the clogging of the printhead. Higher bead densities in the printable range resulted in sensors that were more visible to the naked eyes as there was more signal produced by the color-changing beads. Also, an increase in the bead density slightly reduced the diameter of the fabricated fibers (Figure 2A).

The fiber diameter varied with the loaded bead density, alginate injection rate, and printing speed. The following relationship was used to estimate the surface-to-volume ratio (SVR)

$$SVR = \frac{4}{D} \quad (1)$$

where D is the diameter of fibers. By varying the rate of alginate injection and translational velocity of the extrusion nozzle, while holding the rate of calcium chloride ($CaCl_2$) constant ($30 \ \mu L \ mL^{-1}$), we were able to adjust the diameter of the deposited fibers. The SVR of the printed sensors increased by 27% and 13% when we decreased the flow rate of alginate by 60% and doubled the printing speed, respectively (Figure 2B,C).

Drug-eluting scaffolds were fabricated with two different printing strategies. First, we used the co-axial needle setup to print the structures. However, this method failed for alginate concentrations above 10% w/v because the channels were clogged due to the rapid gelation of alginate at the tip of the printhead. To circumvent this issue, we followed a two-step process in which the gel was first deposited on the printing bed using a single-needle extruder and then was crosslinked by placing a drop of $CaCl_2$ solution on top of the construct. Figure S4A (Supporting Information) summarizes the printability of each printing method, indicating that low-concentration alginate (2–6% w/v) was printable using the one-step process while high-concentration alginate (>10% w/v) required a two-step strategy. Fiber diameter and SVR ratio for 16% w/v alginate were measured using various flow rates and printing speeds. Similar to the low-concentration alginate, the SVR decreased at higher injection rates and slower printing speeds (Figure 2B,C).

One of the main advantages of using hydrogels as a substrate for wound dressings is their ability to retain moisture at the wound site. However, hydrogels are prone to rapid dehydration, which can compromise the integrity of the dressing and ultimately affect its functionality. Rapid dehydration of the hydrogels poses a major challenge for the clinical application of gel-based dressings. We evaluated the dehydration rate of the dermal patch by measuring its weight loss at 37 °C and observed that the alginate patch was completely dehydrated in less than 10 h (Figure S5A, Supporting Information). Influential parameters on dehydration rates including alginate concentration and dressing thickness were altered for these experiments. The dehydration rate was slower when alginate concentration increased from 2% to 4% w/v and patch thickness doubled from 1.5 to 3 mm (Figure S5A, Supporting Information). Blending glycerol with alginate reduced the dehydration rate of the patch significantly and improved its flexibility (Figure 2D,E). While the alginate dressings lost more than 50% of their weight in 3 h, those made from alginate and glycerol only lost 20% of their initial weight during the same period (Figure 2E). Although addition of glycerol slightly reduced the Young's modulus of the dressing (Figure S5B, Supporting Information), it improved the stretchability of the dressing (Figure 2F).

The swelling behavior is a critical parameter in the design of dressings as it determines the capability of the dressing to absorb the exudates and to keep the wound moist. Additionally, the patches are lyophilized for storage and transport and should be hydrated in an aqueous medium prior to use. Therefore, the swelling test will provide the required time for the dressing to reach equilibrium. We evaluated the swelling property of the proposed hydrogel-based dressings by soaking lyophilized patches in phosphate-buffered saline (PBS) and measuring their weight over time. The swelling degree of the dressings was examined for different thicknesses and hydrogel contents (Figure 2G). Thicker dressings exhibited higher swelling degrees while the effect of alginate content was found to be insignificant. Moreover, the time needed for the dressings to reach equilibrium was about 2 h and was independent of the thickness and alginate content of the dressings. Almost an order of magnitude reduction was observed for the dressings that were made from a glycerol and alginate as compared to those that were made from alginate alone (Figure 2H).

Moisture control is an important parameter for promoting the healing process in wounds. [21,22] The control of evaporative water loss in addition to the ability of the dressing to absorb wound exudate is therefore essential for the design of a proper dressing. We performed a water vapor transmission rate (WVTR) assay to quantify the amount of water vapor that can pass through the alginate dressing. We studied the effect of blending glycerol with alginate and covering the dressing with a silicon-based membrane on the WVTR (Figure S5C, Supporting Information). Our results showed that the dressings that were made from pure alginate had the WVTR of 8252 ± 1167 g m^{-2} d^{-1}, while those that were made from a blend of alginate and glycerol exhibited a slightly higher WVTR of 8665 ± 1011 and 9077 ± 1184 g m^{-2} d^{-1} for 20% and 40% w/v glycerol contents, respectively (Figure S5D, Supporting Information).

The biocompatibility of the materials used in the fabrication of GelDerm is the most important factor for the clinical application of the dressing as wounds can be potentially exposed to toxic agents that may exacerbate the healing process. Alginate and glycerol are

biocompatible materials that have been widely used for epidermal applications.[19,23,24] Cabbage juice is a natural compound that is extracted from red cabbage. Although Brilliant Yellow was conjugated to anion-exchange beads and the beads were trapped in alginate fibers, a Live/Dead assay on skin fibroblasts was conducted to ensure the cytocompatibility of the dressing. High cell viability confirmed that the dye did not leach out of the beads and hydrogels (Figure S6, Supporting Information).

2.3. GelDerm Interfaces to a Smartphone and Image Processing

Color-changing sensor arrays were characterized by using ImageJ image processing software and an in-house smart-phone application. Photographic images of the sensors that were exposed to pH buffer solutions in the range of 4.00–9.18 were taken every 10 s (Figure S7A, Supporting Information). These images were then used to generate standard curves for quantifying the pH values. Brilliant Yellow sensors turned orange and red under acidic and alkaline conditions, respectively (Figure 3A). The color of the sensors that were made from cabbage juice changed from purple to green in acidic and alkaline conditions, respectively (Figure 3B). The image-processing analysis was conducted by importing the recorded images in ImageJ and measuring the grayscale intensities of the red, green, and blue (RGB) channels for each sample. The intensities in all channels decreased with increasing pH in sensors made from Brilliant Yellow; blue and red channels had the lowest and highest changes, respectively (Figure S7B, Supporting Information). For the sensors that were made from cabbage juice, the response of the green channel to pH variation was monotonic and the red channel did not follow a trend, while the blue channel represented a relatively consistent decreasing trend in its intensity when pH increased (Figure S7C, Supporting Information). Therefore, red and blue channels were used for producing the standard curves for Brilliant Yellow and cabbage juice, respectively. Overall, cabbage-juice-based sensors had a more noticeable change in color when analyzed with the naked eye. On the other hand, Brilliant-Yellow-based sensors had a larger difference in channel intensity, which is a desirable characteristic for automated image processing. Brilliant Yellow sensors also had a significantly smaller variation in grayscale intensity under the same pH conditions, resulting in reduced standard deviations (SD). Standard polynomial curves were fitted to the red and blue channels' intensity for Brilliant Yellow and cabbage juice sensors, respectively, with grayscale intensity on horizontal axis versus pH on vertical axis as shown in Figure 3C,D. These curves were used to determine the pH of the environment to which the sensors were exposed based on the grayscale intensity derived from analyzing their photographs.

We evaluated the effect of different design parameters including (1) the concentration of alginate in the sensors and in the dressing body, (2) thickness of the dressing body, and (3) SVR of the porous sensors on the response time. The response time was measured by adding a buffer solution with a known pH to the sensors that were initially kept in a neutral environment (pH = 7) and monitoring the color change of the sensors over time. We considered red channel for sensors made from Brilliant Yellow and blue channel for those made from cabbage juice. The time after which the sensors did not show any change in their grayscale intensity was considered as the sensor's response time (Figure 3E). The response time of the sensors was generally fast and the result could be obtained in less than 5 min. No significant difference in the response time of the sensors was observed in different pH

conditions (Figure S8, Supporting Information). However, the concentration of alginate had a considerable influence on the response time of the sensors. In sensors made from Brilliant Yellow, increasing the alginate concentration from 2% to 6% w/v yielded an 85% increase in the response time (Figure 3F). The effect of alginate concentration on the response time of the sensors made from cabbage juice was more pronounced, as sensors made from 6% w/v alginate had a threefold increase in response time as compared to 2% w/v alginate. Similarly, altering the patch structure by changing the alginate concentration from 2% to 6% w/v resulted in considerable changes in response time from 200 to 730 s and from 610 to 1000 s for Brilliant Yellow and cabbage juice, respectively (Figure 3I). Such an increase in the response time could be attributed to the lower porosity and smaller pore size of the alginate at higher concentrations, which hinder the diffusion of H^+ ions through the hydrogel. We also investigated the effect of porosity on the response time of the sensors. Nonporous sensors were made from square sheets of alginate gels with the same dimensions as the porous sensors. Our results showed that porous sensors were considerably faster than the nonporous ones due to the enhanced transport of protons through the matrix, confirming our original hypothesis of using printed sensors (Figure 3G). We also assessed the effect of fiber diameter (SVR) on the response time of the sensors (Figure 3H). As the SVR was increased by decreasing the fiber diameter, faster response time was achieved.

Another parameter that affected the response time of the sensors was the thickness of the dressing. Increasing the thickness from 1.5 to 3 mm resulted in threefold slower response times (Figure 3J). Such an increase in the response time could be attributed to the longer time that was required for thicker dressings to reach equilibrium condition as the H^+ ions were diluted in larger volumes compared to thinner dressings. We confirmed this behavior by analyzing the mass transport in the dressing numerically (Figure S9, Supporting Information). Blending glycerol with alginate further increased the response time of the sensors (Figure 3K).

Based on the characterization results, alginate 4% was chosen to fabricate pH sensors due to the ease of printing and better stability in printed fibers with this concentration. Furthermore, there was no significant difference in pH response time (less than 100 s) between alginate 2% and 4%, as seen in Figure 3F. In contrast, decreasing patch thickness and alginate concentration considerably reduced the pH response time. Moreover, the use of lower alginate concentration with reduced patch thickness resulted in a favorable flexibility to reach a conformal contact between the patch and its substrate as shown in Figure 1E. Therefore, alginate 2% and thickness of 1.5 mm were chosen to fabricate hydrogel patches for the following experiments.

2.4. Colorimetric Detection of Bacterial Infections and Treatment of Infected Wounds Using GelDerm

The performance of GelDerm in the detection pH changes due to the growth of Gram-positive *S. aureus* and Gram-negative *P. aeruginosa* was evaluated. Both strains are highly prevalent in the wounds and infections caused by these pathogens remain a common complication in acute and chronic wounds.[19] We assessed the ability of GelDerm to detect pH changes due to bacterial activity visually and by taking images with a smart-phone.

Supernatants from the bacterial cultures were collected every 1 h for 18 h, and a droplet of the culture media was placed on the sensors. After 10 min, an image of each sample was taken by a smartphone camera for further quantification. For the samples that were collected from *P. aeruginosa* cultures, the pH was slightly acidic at the beginning (pH = 6.5) and became more alkaline as the culture continued for 18 h (pH = 9.0) (Figure 4A-i). However, the trend of pH change in *S. aureus* samples was the opposite, and the samples became more acidic up to 8 h (pH $\approx$ 6.0) and then became neutral after 18 h of culture (pH = 7.0) (Figure 4A-ii). A visible color change was observed in sensors when the pH variations were more than one unit. This change was more pronounced in the sensors that were made from cabbage juice. However, smaller pH variations were not visually detectable.

The recorded images were analyzed to quantify the color changes of the sensors that were exposed to bacterial cultures at different time points. After wirelessly collecting the images, we performed a digital image processing in ImageJ to assess the variations in grayscale intensity in the red and blue channels for Brilliant Yellow and cabbage juice, respectively. An imaging box was used to achieve uniform environmental lighting. The actual pH of the solutions was measured using a commercial electrochemical pH probe as the reference. Figure 4B shows the variation of the actual pH values in the samples that were collected from *P. aeruginosa* cultures. A linear increase in the pH was observed for the first 8 h and the samples became more alkaline. The pH value changed in the range of 6.5–9. For this range, we achieved a ± 10% accuracy for the colorimetric readings compared to the reference pH values that were measured by the electrochemical probe (Figure 4C). While the color change in the sensors with cabbage juice was more visible to the human eye, Brilliant Yellow yielded more accurate pH measurements, with an error below 4% compared to an error of 9% from the cabbage juice sensors, as indicated in Figure 4D. pH variations in the samples collected from *S. aureus* cultures were analyzed using a similar colorimetric method and compared with the reference electrochemical values. Samples from *S. aureus* cultures were more acidic and were in the range of 6–7.5. However, the trend was different than *P. aeruginosa* as the pH did not change significantly for the first 3 h, then dropped about one unit in 2 h, and finally reached a plateau afterward (Figure 4E). The accuracy of the sensors was slightly lower in the acidic environment (Figure 4F) with an error of <6% for Brilliant Yellow and <14% for cabbage juice, indicating a higher accuracy for Brilliant Yellow in acidic condition as well (Figure 4G).

We performed an ex vivo test to demonstrate the ability of GelDerm in the colorimetric detection of bacterial infection. Pig skins were inoculated with *P. aeruginosa* at different initial densities of 1.4×10^5, 1.4×10^6, and 1.4×10^7 CFU cm^{-2}. After 12 h, GelDerm was placed on the infected skins, and the color change in the sensors was inspected visually and by using the image processing approach. We observed a clear color change in infected samples, which was more pronounced in samples that were inoculated with higher initial bacterial densities (Figure 5A). The increase in the pH of the infected skins was confirmed by commercially available pH strips. We also used a smartphone to quantify the pH values of the infected skins (Figure 5B) and compared these results with the readings of the pH strips (Figure 5C).

To examine the antibacterial effectiveness of the drug-eluting scaffolds, we performed a semiquantitative bacteria inhibition assay using *P. aeruginosa*. To identify an effective dosage of gentamicin to completely eradicate the bacteria, scaffolds with the same volume were loaded with 50–300 mg mL^{-1} of the drug. Scaffolds with no drugs and filter paper impregnated with the same amount of drugs were used as negative and positive controls, respectively. Gentamicin is widely used as an effective antibiotic agent against a wide range of Gram-negative and Gram-positive bacteria, including *P. aeruginosa*.[25–27] Our results suggested that the loading dosages of less than 200 mg mL^{-1} were not effective in eradicating the bacteria (Figure 5D-i). Scaffolds with a loading dosage of 200 mg mL^{-1} formed a ring that outlined the inhibited zone around the drug-eluting patch, while the areas under both control patch regions still had bacterial growth. The observed white ring around the scaffold within the inhibited zone was suspected to be infected by the bacteria. Therefore, we collected swab samples from three different zones near the scaffold (point 1), in the white region (point 2), and at the edge of the ring (point 3), then plated the samples overnight on another agar plate. Figure 5D-ii demonstrates that there were no bacteria within the proximity of the patch and a few colonies of bacteria formed in point 2, while a large number of colonies formed from the samples collected at the edge of the ring. These results are consistent with typical drug diffusion within agar plates that leads to higher concentrations of the drug at the vicinity of the scaffold and lower concentrations away from the scaffold. The formation of the white ring around the scaffold can be attributed to the interaction of the phosphate ions in the agar and calcium ions that were releasing from the calcium alginate scaffolds. Then negative controls (scaffolds with no drugs) did not inhibit the bacterial growth while the positive control (drug + filter paper) formed a clear inhibition ring around the filter paper (Figure 5D-iii).

An additional ex vivo test was conducted to observe the effect of bacterial growth on the color change of pH sensors with the incorporation of drug release. In this experiment, pig skin samples were inoculated with *P. aeruginosa* with the density of 1.4×10^7 CFU cm^{-2}. Hydrogel dressings with three different concentrations of gentamicin—0 (no drug), 0.5 mg mL^{-1} (low concentration), and 2 mg mL^{-1} (high concentration)—were placed on the skin samples from the beginning of the experiment, and dynamic pH change was observed by real-time photography inside the incubator for 15 h. Figure 5E shows that the variation of pH was higher in dressings without the antibiotic agent, but was reduced when the drug was incorporated in the dressing in a dose-dependent manner.

To examine the functionality of the developed wound dressing in detecting infections with a mixture of bacteria, a similar ex vivo experiment with real-time photography was conducted with a 1:1 mixture of *P. aeruginosa* and *S. aureus*. As shown in Figure 5F a trend of pH change—starting from 7.1 and reaching a plateau of about 7.8—can be related to the presence of bacteria on the skin samples.

2.5. Integration of GelDerm with Commercial Dressings

We assessed the ability to integrate GelDerm with commercial dressings. Figure 6A shows a fabricated hydrogel dressing attached to a Mepitel dressing. Mepitel is a wound dressing with the contact layer that has a transparent silicon mesh that allows the transport of oxygen

to the wound site, while reducing the evaporation rate from the wound. Moreover, the transparency of the thin membrane enables colorimetric detection of pH variations in the wound. Furthermore, this dressing contains an adhesive layer that ensures proper attachment of the dressing to the tissue. These dressings are flexible and can conform to the curved surfaces of the skin (Figure 6A, inset).

We developed an in-house application (iDerm) to record color changes in the sensors and convert them into quantitative data. Figure 6B shows the process of taking images using a smartphone, selecting the sensors by the user, and displaying the final results on the screen. iDerm split the red, green, and blue channels and used a grayscale in the red and blue channels to quantify the pH values for Brilliant Yellow and cabbage juice sensors, respectively. Reference color markers (blue and red) were used to eliminate the dependence of the results on different lighting conditions, which may occur in practical applications. A long touch feature was designed in the application that allowed the user to select each sensor by holding a finger on the image of the senor on the screen for few seconds (see Video S1 in the Supporting Information). A user-friendly interface was designed to display the final results on the screen and record the pH values for continuous monitoring of the wound condition. The recorded data were uploaded on a secure Cloud storage drive that would allow medical personnel to access the patient data and monitor the wound condition in real time.

We evaluated the ability of the sensors to detect pH variations on biological tissues by placing the Mepitel/hydrogel dressing on pig skins, which were sprayed with different buffer solutions (Figure 6C). Color change was visible between the acidic, neutral, and basic conditions. However, more accurate results were obtained through the use of smartphone image acquisition and image processing. We placed the dressing on the epidermis and dermis layers of pig skins to investigate the effects of tissue color on the readings. The errors in readings in dermis and epidermis were below 10% and did not depend on the color of dermis and epidermis layers (Figure S10, Supporting Information).

We studied the effect of Mepitel on the dehydration rate of the hydrogel dressing. Dressings with 2% w/v alginate were covered by Mepitel and their weight were measured in 24 h. The effect of Mepitel on the dehydration rate of the hydrogel dressings was significant (Figure 6D). Hydrogel dressings that did not have Mepitel lost 90% of its water content after 24 h, those that were covered by the commercial dressing only lost 50% of their water content. Furthermore, covering the dressing with Mepitel significantly reduced the WVTR to 2218 $\pm$ 52 g m^{-2} d^{-1}.

3. Discussion

The multifunctional dressing introduced here (GelDerm) represents a colorimetric pH sensing array and drug-eluting scaffold that can be used for detecting and treating infections at the wound site. Compared to existing wound dressings, GelDerm is unique in the sense that it has both diagnostic and therapeutic components integrated into a single dressing. This multifunctional dressing will generate significant savings in healthcare costs, due to reduced clinical inspection time, the elimination of the unnecessary changing of dressings in patients

who are suspected to have infections, and shorter hospital stays resulted from faster wound healing. Additionally, higher dosages of the antibacterial agent can be used without imposing adverse side effects to other organs due to the localized delivery of the drug at the site of injury. The introduced dressing is composed of alginate and glycerol, which are approved by the US Food and Drug Administration for wound healing applications.[28] The addition of hydrogels helps maintaining a moist environment for the wound and promotes the healing process by up to 50% compared to the wounds that are only exposed to air.[29] Additionally, GelDerm can be integrated within a commercially available dressing such as Mepitel and placed on the wound without chemical or physical irritation.

The soft mechanical properties and ability for GelDerm to conform to biological surfaces with irregular curvatures were analyzed. Moreover, we studied the biocompatibility of the constituent materials, antibacterial properties, and hydration and evaporative characteristics of the dressing. The ability to digitally analyze colorimetric responses as well as integrate GelDerm within commercially available dressings was also realized. First, the fabrication process of the sensors and their ability for colorimetric detection of pH variations due to bacterial infections were systematically investigated. We hypothesized that using porous sensors would yield to faster response times due to the higher available SVR. 3D printing was used in this work as a versatile approach for fabricating complex structures in a high-throughput manner.[30,31] This method enabled us to print each porous sensor in less than a minute. The ability to print sensors allows scaling up the process for making large-scale dressings that can cover larger wound areas. The SVR of the fabricated sensors was a function of the diameter of fibers and the spacing between them. The diameter of the fiber was altered by adjusting the flow rate of extruded alginate and the nozzle translational speed. Increasing the flow rate of the extruded alginate resulted in the deposition of more material, which resulted in fibers with larger diameters. In contrast, increasing the nozzle speed resulted in smaller fiber diameters as less material was deposited per unit length of the fibers. A similar trend was reported by others in previous studies.[32,33] Another parameter that affected the diameter of the fibers was the density of the encapsulated color-changing beads. Our results suggested that higher concentrations of the beads resulted in a decreased fiber diameter. Higher concentrations of the bead resulted in stronger signals, which facilitated the colorimetric detection of the pH variations.

In bacterial infections, the variation of pH depends on the species. For example, we demonstrated that the pH of *P. aeruginosa* cultures increased as the bacteria was growing while the pH decreased with culture time for *S. aureus*. *S. aureus* is a facultative anaerobe and grows best in an aerobic environment. Its metabolism is both respiratory and fermentative, and can ferment a variety of carbohydrates (like glucose) to produce acidic end products.[34] *P. aeruginosa*, on the other hand, is not fermentative and has a strictly aerobic respiration. It utilized peptones in the media to produce alkaline end products.[35] In current practice, the dressing is changed on regular basis; swab samples are collected in suspected patients; and the patient is treated with systemic antibiotics to prevent possible infections.[29] However, this method is painful, time-consuming, and labor intensive. GelDerm uses pH as a marker of bacterial infections and utilizes a colorimetric method with the ability to interface with smartphones. Our approach enables the healthcare personnel or the patient to monitor the pH of the wound over time and change the dressing when infection is detected.

For the fabrication of the sensors, ion-exchange beads were doped with pH indicators that undergo a color change in response to the variation of the acidity of the environment. The electrostatic interaction between the dye and the beads minimized the leakage of the dye from the beads.[36] Encapsulation of the beads within the hydrogel fibers ensures that the beads do contact the skin and disperse within the wound site. Using this method, pH values in the range of 4.0–9.0 were visually detectable by means of a smartphone. Although the sensitivity of visual detection was one pH unit, analyzing the images taken by smartphones improved the sensitivity to less than 0.5 pH units. Such a sensitivity could be potentially used for early detection of bacterial infection in the first few hours (according to our data shown in Figure 5). We achieved the sensitivities as small as ± 5% (maximum: ± 0.45 pH units for the pH of 9.0) when the measured values were compared to the readings of an electrochemical pH probe. We characterized the effect of design parameters including the fiber diameter, concentration of alginate, and the thickness of the dressing on the response time of the sensors. The fastest response time achieved in this work was 5 min, and this time was increased due to higher diffusive barriers against the transport of ions within the sensors as the fiber diameter, hydrogel concentration, and the thickness of dressing increased (Figure 3). It is noteworthy that the response time of a nonporous sensor was significantly higher than the printed sensor by a factor of 3, which confirmed our hypothesis in using porous sensors.

The ability to uptake the body fluid is essential for the maintenance of the moist wound environment.[37] Hydrogels are polymeric networks that can uptake water up to thousands of times of their dry weight;[38] therefore, they are considered as suitable dressing materials for wound management. Among all hydrogels, alginate is a naturally derived polysaccharide that has been extensively used for drug delivery, tissue engineering, and wound dressings. [14,18,39] Alginate is a natural hemostat that can be used to prevent bleeding at the wound site. This hydrogel also does not adhere to tissues; thus, removing the dressing from the wound does not cause much trauma, and reduces the pain experienced by the patient during dressing changes.[16] However, alginate dehydrates rapidly and loses its flexibility upon dehydration. Therefore, we added glycerol to alginate to reduce the dehydration rate by 30%. Moreover, dressings that were made from glycerol maintained their mechanical integrity and flexibility after complete dehydration. When we combined GelDerm with Mepitel, the rate of dehydration was significantly decreased due to reduced evaporation caused by the silicon membrane of the commercial dressing. Therefore, combined GelDerm/ Mepitel dressing holds a great promise for treatment of chronic wounds as it can stay on the wound over longer periods as compared to the current gel-based dressings.

Diagnostics and effective management of an infection are critical for the success of any wound dressing. Current dressings with antibacterial properties do not have the ability to detect infections at the wound site. As a result, visual inspection of the wound condition by skilled personnel is needed, which is cumbersome, painful, and requires the change of dressings on a daily basis. The proposed multifunctional dressing is capable of measuring pH as a marker of bacterial infection and delivering antibacterial agents. We developed an in-house smartphone application (iDerm) that records the digital images of GelDerm and reports the pH values. iDerm enables the patient to record the wound condition at home and relay the information to the healthcare personnel, who can make decisions on the subsequent

treatment strategies. We demonstrated the ability of GelDerm in the colorimetric detection of bacterial infections using *in vitro* and ex vivo tests. First, we cultured two of the most prevalent strains of bacteria, i.e., *P. aeruginosa* and *S. aureus*, that are found in infected wounds and measured the pH of the culture medium over 18 h using GelDerm and a commercially available pH probe. GelDerm was able to detect pH variations in the culture media with less than ± 5% error, indicating the accuracy of our colorimetric approach. Then, we infected pig skins with bacteria for 12 h and measured the pH changes on the samples using GelDerm and commercially available pH strips. A clear change in the color of the sensors was observed in the infected skins as compared to the control. This color change was more substantial in samples that were infected with higher initial inoculation densities of the bacteria.

Topical delivery of antibiotics minimizes the complications of intravenous administration of the drug and offers the advantage of delivering increased drug concentrations directly to the wound site. We encapsulated gentamicin, which has a wide spectrum of activity against most bacteria strains that are found in infected wounds, in the drug-eluting scaffolds.[40] The rationale behind using drug-eluting scaffolds was to provide a more localized delivery of the drug at the interface of the wound and dressing. Releasing antibiotics at the wound site sterilizes the wound after the dressing is placed on the injury. Our in vitro inhibition assay for *P. aeruginosa,* as a model bacterium, demonstrated the effectiveness of the topical delivery of gentamicin at 3 mg mL^{-1} dosage. These dressing also showed no toxicity in contact with human primary keratinocytes and fibroblasts, making them a suitable candidate for treatment of dermal injuries.

4. Conclusion

Overall, the proposed technology holds great promise in managing chronic and acute injuries caused by trauma, surgery, or diabetes. The ability to diagnose and treat the infections at the site of injury reduces manual inspection of the wound and systemic administration of antibiotics to the patients. With the formulation that we used in the design and fabrication of the proposed multifunctional dressing, it can be lyophilized and sterilized for long-term storage without losing flexibility, antibacterial efficacy, and ability to detect pH changes at the wound site. Our efforts are now focused on improving the performance of this system by integrating more sensing elements within the dressing to detect more specific bacterial markers. We are also investigating the use of more advanced biomaterials that possess stronger mechanical properties in terms of flexibility and moisture management for longer periods.

5. Experimental Section

Preparation of Brilliant Yellow and Cabbage Juice Loaded Beads

About 135 mg of Brilliant Yellow dye (TCI, Tokyo, Japan) was dissolved in 6 mL of ethanol; 24 mL of DI water was then added, and the solution was stirred for 30 min. Cabbage juice was prepared by adding 15 g of chopped red cabbage to 30 mL of DI water, keeping at 90 °C for 1 h, and filtering to obtain ≈30 mL of the final solution. About 3378 mg of Dowex 1 × 4 chloride form (Sigma, St. Louis, USA) was added to 50 mL of DI water in a

Falcon tube, and it was manually stirred, then settled until the beads were at rest on the bottom of the tube. The water content was carefully extracted with a pipette and replaced. This step was repeated twice with DI water and once with anhydrous ethanol. After washing, 30 mL of DI water was added to the beads and the obtained suspension was added to the dye solution (Brilliant Yellow solution or cabbage juice). Supernatant was washed multiple times to obtain a clear supernatant.

Preparation of Alginate Solutions for Sensors and Drug-Eluting Scaffolds

For sensors, DI water was added to pH-sensitive beads to reach the final volume of 15 mL. For drug-eluting scaffolds, a desired amount of gentamicin sulfate (according to the drug content in the final scaffold) was added to 5 mL of DI water. Sodium alginate (Sigma, St. Louis, USA) was then added to both bead suspension and drug solution to achieve the desired concentration, kept at 60 °C for 1 h, and vortexed periodically at 3000 rpm.

3D Printing and Characterization of Sensors and Drug-Eluting Scaffolds

A commercial 3D printer (Prusa i3) was modified by incorporating a microextruder to print hydrogel fibers. To print alginate 2–6% w/v, a microextruder that consisted of a coaxial needle system was powered by two syringe pumps (Harvard Apparatus) to deliver alginate with different concentration (90 μL) min^{-1} and $CaCl_2$ (6% w/v, 30 μL min^{-1}) (Bio Basic, Inc., Toronto, Canada) solutions. Alginate was ionically crosslinked at the tip of the extruder and deposited on the 3D bioprinter's bed. A single extruder was used for printing 16% w/v alginate with a flow rate of 22 μL min^{-1} and 5 mm s^{-1} printing speed in normal condition. Mentioned flow rates and printing speeds were altered for characterization based on different parameters. Printed scaffolds were then observed under a light microscope (Olympus IMT-2, Tokyo, Japan) to measure the individual fiber diameters.

Analysis of pH-Sensitive Sensors' Response to Different pH Environments

For testing the response time and RGB color intensity of the pH-sensitive components, a light diffusing box was built, with a camera on top that took a photo automatically in 5 s intervals. This device was used to test pH sensors with different properties such as alginate concentrations, fiber diameters, and pH of the solutions that the sensors were exposed to. The individual images were then analyzed using ImageJ software. The images were converted to grayscale format of each individual RGB channel, and their change in intensity was measured to determine the time for each sensor to reach a steady-state condition.

Fabrication of the Dressings

About 1 mL of alginate solution (2% w/v for normal condition) was spread on a cuboid 35 mm × 55 mm × 1.5 mm mold. Four pH sensors were placed at the corners, and two drug-eluting scaffolds were placed at the center. About 2 mL of alginate solution (2% w/v) was then added to the mold; an agarose sheet (agarose: 1.5% w/v, $CaCl_2$: 4% w/v) was placed on top and left for 20 min to crosslink. After removing the sheet, the crosslinked patch was removed from the mold.

Exposing the Sensors to Bacteria Supernatant

A strain of *P. aeruginosa* ATCC 10145 was cultured in Tryptic soy broth (TSB, Fluka Analytical), and 1 mL of the supernatant was collected every hour. About 150 μL of each supernatant was deposited on different pH sensors to do the photography and subsequent assessments.

Ex Vivo Bacterial Detection Tests

Noninjured samples of pig skin were cut into four portions of area 25 cm^2, disinfected with 70% v/v ethanol, and washed with saline solution. To reach the dermis layer, the epidermis layer was carefully removed by a sterile razor blade until the dermis layer was observed. The skin portions were individually transferred into sterile Petri dishes. Before inoculating the skins with bacteria, a swab sample was taken from skins and plated on a Tryptic soy agar (TSA, Sigma-Aldrich) plate for 24 h to ensure that the skin samples were properly sterilized. An aliquot of 200 μL of an overnight culture of *P. aeruginosa* was deposited on the skins and distributed over the skin using a glass spreader. Four conditions of no bacterial infection (control) and three initial inoculation densities of 1.4×10^5, 1.4×10^6, and 1.4×10^7 CFU cm^{-2} were considered. The infected skins were then incubated at 37 °C in a moist atmosphere. After 12 h, GelDerm was placed on the samples, and images were taken by a smartphone after 30 min to analyze the sensors. For measuring pH on pig skin, buffer solutions with pH 4.00 (VWR Analytical), 6.86 (Fisher Scientific), and 9.18 (Fisher Scientific) were sprayed on three slices of pig skin. Patches of both types, Brilliant Yellow and cabbage juice, were put over the pig skin and photographic images were taken after 10 min for subsequent analysis.

Bacteria Viability Loss Assay

Drug-eluting scaffolds were embedded in alginate patches as described previously; patches were then placed on top of a TSA plate on which *P. aeruginosa* bacteria were spread, and the effect of the antimicrobial was investigated after incubation at 37 °C for 18 h.

Mechanical Test

Rectangular alginate/glycerol sheets (20 mm × 10 mm × 2 mm) made of alginate 2% w/v and alginate 2% w/v + glycerol 20% w/v were prepared by crosslinking with agarose sheets containing CaCl$_2$ similar to the preparation of the patches. The samples were kept in PBS and their tensile properties were measured using an Instron 5542 mechanical tester. The fibers were sandwiched between the grips and were stretched at a constant strain rate of 0.1 mm min^{-1}. The fibers were kept hydrated using an ultrasonic humidifier during the test, and four samples for each type were tested. The Young's modulus was calculated using the slope of the stress–strain curve and the strain rate.

Dehydration and Hydration Tests

Square gel sheets (15 mm × 15 mm) made of two different concentrations of alginate (2% and 6% w/v) and two different thicknesses (1.5 and 3 mm) were fabricated by crosslinking with agarose sheets containing CaCl$_2$, similar to preparation of the patches. Four samples of each condition were prepared for the dehydration and hydration tests. The dehydration test

was conducted by keeping samples in ambient room temperature, then measuring the weight during definite time intervals of 48 h. The remaining mass was subtracted from its initial value for each sample. For the hydration test, samples were first frozen at −80 °C for 24 h, lyophilized for 72 h, weighted, and immersed in PBS. The weight was then recorded during definite time intervals of 3 h, and the degree of swelling was then obtained by determining the gained weight for each sample.

Cell Culture

Human primary keratinocytes and fibroblasts were harvested according to the previously described method[21] from foreskin samples derived from healthy patients receiving circumcision. Keratinocytes were cultured in keratinocyte serum-free medium (Invitrogen Life Technologies, Carlsbad, CA, USA) supplemented with epidermal growth factor (0.2 ng mL^{-1}, GIBCO) and bovine pituitary extract (25 ng mL^{-1}). Dulbecco's Modified Eagle's Medium (GIBCO, Grand Island, NY, USA) with 10% fetal bovine serum were used to culture fibroblasts. For all experiments in this study, keratinocytes and fibroblasts at 4–7 passages were used.

Live/Dead, Viability/Cytotoxicity Assay

Cells were cultured in six-well plates with a density of 250×10^3 cells per well. Kynurenic acid with increasing concentration from 50 to 150 μg mL^{-1} was used in the cell media. Cell viability was assessed using Live/Dead assay kit for mammalian cells (Invitrogen) by flow cytometry after 3 d of incubation. In this assay, dead cells and those in apoptosis stage were stained by ethidium homodimer (EthD-1), a red fluorescent nucleic acid dye. On the other hand, live cells can be observed by calcein AM, which is turned to a green fluorescent compound by active intracellular esterase in live cells.

Statistical Analysis

One-way analysis of variance with the Tukey posthoc test was performed on experiments with more than two test groups. Standard deviation was the measure of uncertainty in all data. Error bars indicate the standard deviation of three replicates per data point ($n = 3$). All statistical analysis and graphing were performed with Microsoft Excel.

Supplementary Material

Refer to Web version on PubMed Central for supplementary material.

Acknowledgments

References

1. Mohammadi MH, Heidary Araghi B, Beydaghi V, Geraili A, Moradi F, Jafari P, Janmaleki M, Valente KP, Akbari M, Sanati-Nezhad A. Adv Healthcare Mater. 2016; 5:2459.

2. Church D, Elsayed S, Reid O, Winston B, Lindsay R. Microbiol Rev. 2006; 19:403.

3. Tredget EE, Shankowsky HA, Rennie R, Burrell RE, Logsetty S. Burns. 2004; 30:3. [PubMed: 14693082]

4. Bloemsma GC, Dokter J, Boxma H, Oen IMMH. Burns. 2008; 34:1103. [PubMed: 18538932]

5. Kim DH, Lu N, Ma R, Kim YS, Kim RH, Wang S, Wu J, Won SM, Tao H, Islam A, Yu KJ, Kim T, Chowdhury R, Ying M, Xu L, Li M, Chung HJ, Keum H, McCormick M, Liu P, Zhang YW, Omenetto FG, Huang Y, Coleman T, Rogers JA. Science. 2011; 333:838. [PubMed: 21836009]

6. Huang X, Liu Y, Chen K, Shin WJ, Lu CJ, Kong GW, Patnaik D, Lee SH, Cortes JF, Rogers JA. Small. 2014; 10:3083. [PubMed: 24706477]

7. Najafabadi AH, Tamayol A, Annabi N, Ochoa M, Mostafalu P, Akbari M, Nikkhah M, Rahimi R, Dokmeci MR, Sonkusale S. Adv Mater. 2014; 26:5823. [PubMed: 25044366]

8. Liu Y, Norton JJS, Qazi R, Zou Z, Ammann KR, Liu H, Yan L, Tran PL, Jang KI, Lee JW. Sci Adv. 2016; 2:e1601185. [PubMed: 28138529]

9. Mostafalu, P., Akbari, M., Alberti, KA., Xu, Q., Khademhosseini, A., Sonkusale, SR. Microsyst Nanoeng. 2016. p. 2https://doi.org/10.1038/micronano.2016.39

10. Dargaville TR, Farrugia BL, Broadbent JA, Pace S, Upton Z, Voelcker NH. Biosens Bioelectron. 2013; 41:30. [PubMed: 23058663]

11. Koh A, Kang D, Xue Y, Lee S, Pielak RM, Kim J, Hwang T, Min S, Banks A, Bastien P. Sci Transl Med. 2016; 8:366ra165.

12. Gethin G. Wounds. 2007; 3:52.

13. Schneider LA, Korber A, Grabbe S, Dissemond J. Arch Dermatol Res. 2007; 298:413. [PubMed: 17091276]

14. Lee KY, Mooney DJ. Prog Polym Sci. 2012; 37:106. [PubMed: 22125349]

15. Jain D, Bar-Shalom D. Drug Dev Ind Pharm. 2014; 40:1576. [PubMed: 25109399]

16. Paul W, Sharma CP. Trends Biomater Artif Organs. 2004; 18:18.

17. Murakami K, Aoki H, Nakamura S, Nakamura S, Takikawa M, Hanzawa M, Kishimoto S, Hattori H, Tanaka Y, Kiyosawa T, Sato Y, Ishihara M. Biomaterials. 2010; 31:83. [PubMed: 19775748]

18. Bagherifard S, Tamayol A, Mostafalu P, Akbari M, Comotto M, Annabi N, Ghaderi M, Sonkusale S, Dokmeci MR, Khademhosseini A. Adv Healthcare Mater. 2016; 5:175.

19. Maral T, Borman H, Arslan H, Demirhan B, Akinbingol G, Haberal M. Burns. 1999; 25:625. [PubMed: 10563689]

20. Lavorgna M, Piscitelli F, Mangiacapra P, Buonocore GG. Carbohydr Polym. 2010; 82:291.

21. Bishop SM, Walker M, Rogers AA, Chen WY. J Wound Care. 2003; 12:125. [PubMed: 12715483]

22. Okan D, Woo K, Ayello EA, Sibbald G. Adv Skin Wound Care. 2007; 20:39. [PubMed: 17195786]

23. Yang X, Yang K, Wu S, Chen X, Yu F, Li J, Ma M, Zhu Z. Radiat Phys Chem. 2010; 79:606.

24. Corkhill PH, Hamilton CJ, Tighe BJ. Biomaterials. 1989; 10:3. [PubMed: 2653447]

25. Yetim I, Özkan OV, Dervi oglu A, Erzurumlu K, Canbolant E. J Int Med Res. 2010; 38:1442. [PubMed: 20926017]

26. Chang WK, Srinivasa S, MacCormick AD, Hill AG. Ann Surg. 2013; 258:59. [PubMed: 23486193]

27. Mavros MN, Mitsikostas PK, Alexiou VG, Peppas G, Falagas ME. J Thorac Cardiovasc Surg. 2012; 144:1235. [PubMed: 22819366]

28. Sun J, Tan H. Materials (Basel). 2013; 6:1285. [PubMed: 28809210]

29. Davidson JR. Vet Clin North Am Small Anim Pract. 2015; 45:537. [PubMed: 25744144]

30. Pedde RD, Mirani B, Navaei A, Styan T, Wong S, Mehrali M, Thakur A, Mohtaram NK, Bayati A, Dolatshahi-Pirouz A. Adv Mater. 2017; 29:1606061.

31. Memic A, Navaei A, Mirani B, Cordova J, Aldhahri M, Dolatshahi-Pirouz A, Akbari M, Nikkhah M. Biotechnol Lett. 2017; 39:1279. [PubMed: 28550360]

32. Ghorbanian S, Qasaimeh MA, Akbari M, Tamayol A, Juncker D. Biomed Microdevices. 2014; 16:387. [PubMed: 24590741]

33. Miller JS, Stevens KR, Yang MT, Baker BM, Nguyen DHT, Cohen DM, Toro E, Chen AA, Galie PA, Yu X. Nat Mater. 2012; 11:768. [PubMed: 22751181]

34. Fuchs S, Pané-Farré J, Kohler C, Hecker M, Engelmann S. J Bacteriol. 2007; 189:4275. [PubMed: 17384184]

35. Dawes EA, Ribbons DW. Annu Rev Microbiol. 1962; 16:241. [PubMed: 14025574]

36. Chen Y, Zilberman Y, Mostafalu P, Sonkusale SR. Biosens Bioelectron. 2015; 67:477. [PubMed: 25241151]

37. Queen D, Gaylor JDS, Evans JH, Courtney JM, Reid WH. Biomaterials. 1987; 8:367. [PubMed: 3676423]

38. Seliktar D. Science. 2012; 336:1124. [PubMed: 22654050]

39. Akbari M, Tamayol A, Laforte V, Annabi N, Najafabadi AH, Khademhosseini A, Juncker D. Adv Funct Mater. 2014; 24:4060. [PubMed: 25411576]

40. Junker JPE, Lee CCY, Samaan S, Hackl F, Kiwanuka E, Minasian RA, Tsai DM, Tracy LE, Onderdonk AB, Eriksson E. Plast Reconstr Surg. 2015; 135:151. [PubMed: 25539303]
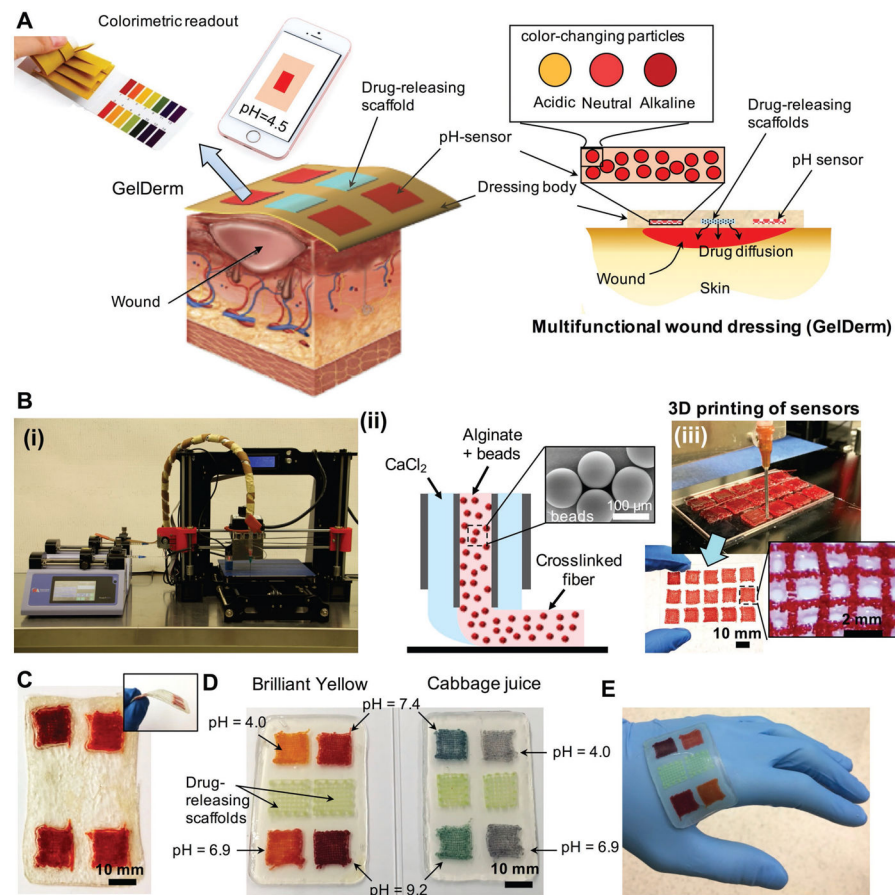
Figure 1.
An advanced multifunctional dressing (GelDerm) for monitoring and management of wounds. A) Schematic representation of GelDerm treatment of epidermal wounds, with pH-sensitive and drug-eluting components. B-i) Porous sensors were fabricated using a 3D bioprinter equipped with a co-axial flow microfluidic nozzle (i). B-ii) Schematic of fiber deposition using the co-axial flow system. B-iii) 3D printer can be programmed to produce arrays of porous sensors for fabrication of large-scale dressings. C) Dressings can be lyophilized and sterilized for storage and transportation. D) Synthetic Brilliant Yellow and naturally derived cabbage juice were used as model pH indicators for the fabrication of the sensors. Sensor arrays enable detecting spatial variations of pH on the wound site. Drug-eluting scaffolds release high doses of antibiotics at the wound site to eradicate the bacteria that may remain on the wound site each time the dressing is replaced. E) GelDerm can maintain a conformal contact with irregular surfaces.
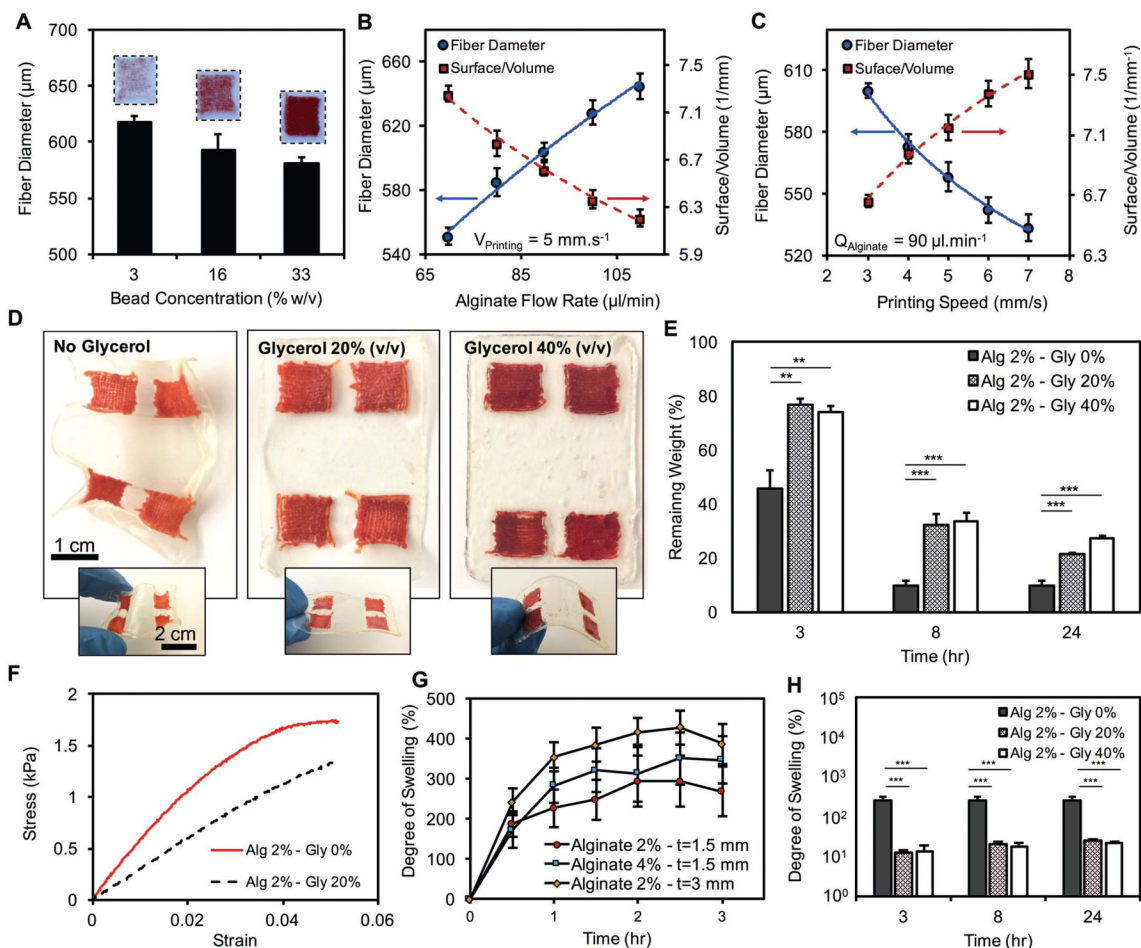
Figure 2.
Characterization of the fabrication process of GelDerm and its physical properties. A) Effect of bead concentration on the diameter of printed fibers. Higher bead densities resulted in darker colors. During the extrusion and 3D printing of the sensors, fiber diameter and surface -to-volume ratio was controlled by adjusting B) alginate flow rate, and C) the travel speed of the nozzle. D) Effect of blending glycerol with alginate on the mechanical integrity and flexibility of the dressings. E) Addition of glycerol to alginate reduced the dehydration rate of the dressing significantly. F) Stress–strain curve for dressing made from pure alginate and alginate–glycerol blend. G) Degree of swelling of the dressings as a function of alginate concentration and thickness. H) Addition of glycerol to alginate reduced the degree of swelling significantly. Error bars represent the SD ($n = 3$); $**p < 0.005$ and $***p < 0.0005$.
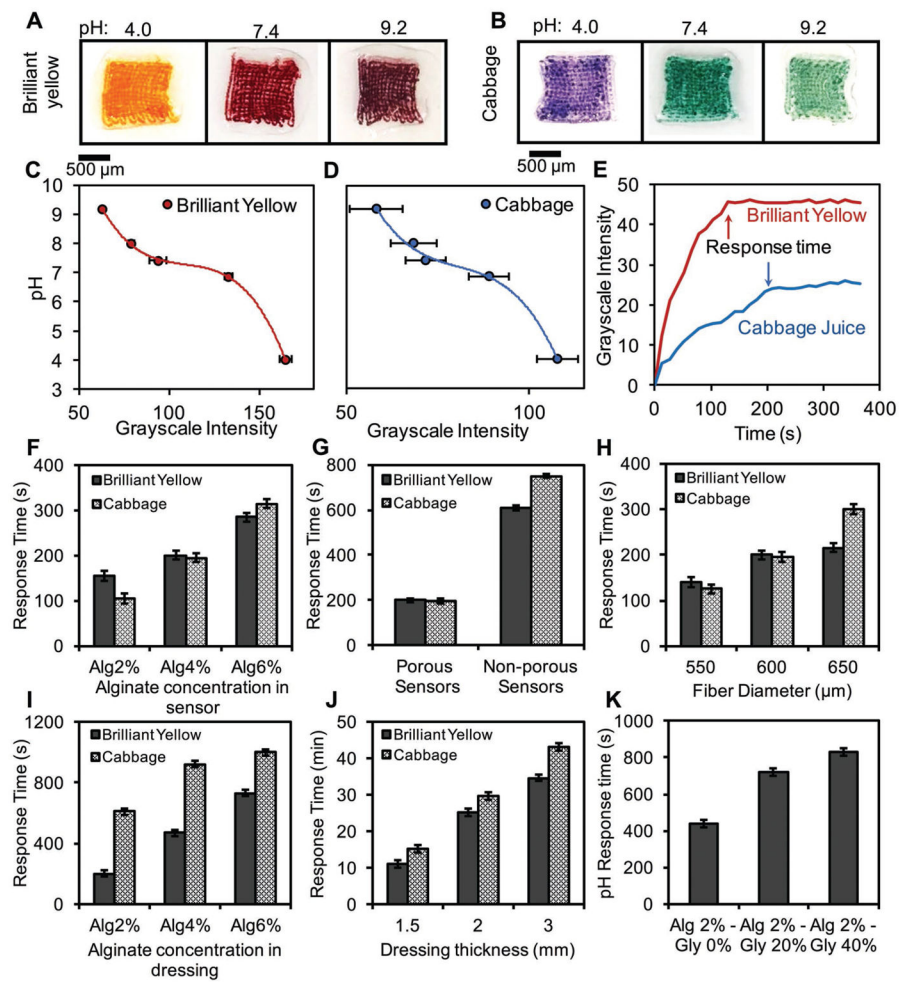
Figure 3.
Quantitative colorimetric analysis of pH using porous sensors. Colorimetric detection of pH using A) Brilliant Yellow and B) cabbage juice. Standard calibration curves for sensors made from C) Brilliant Yellow and D) cabbage juice. E) Typical response times of porous sensors. Effect of F) alginate concentration in the sensors, G) sensor porosity, H) diameter of sensor fibers, I) alginate concentration in the dressing body, J) thickness of the dressing, and K) glycerol content and on the response time. Error bars represent the SD ($n = 3$).
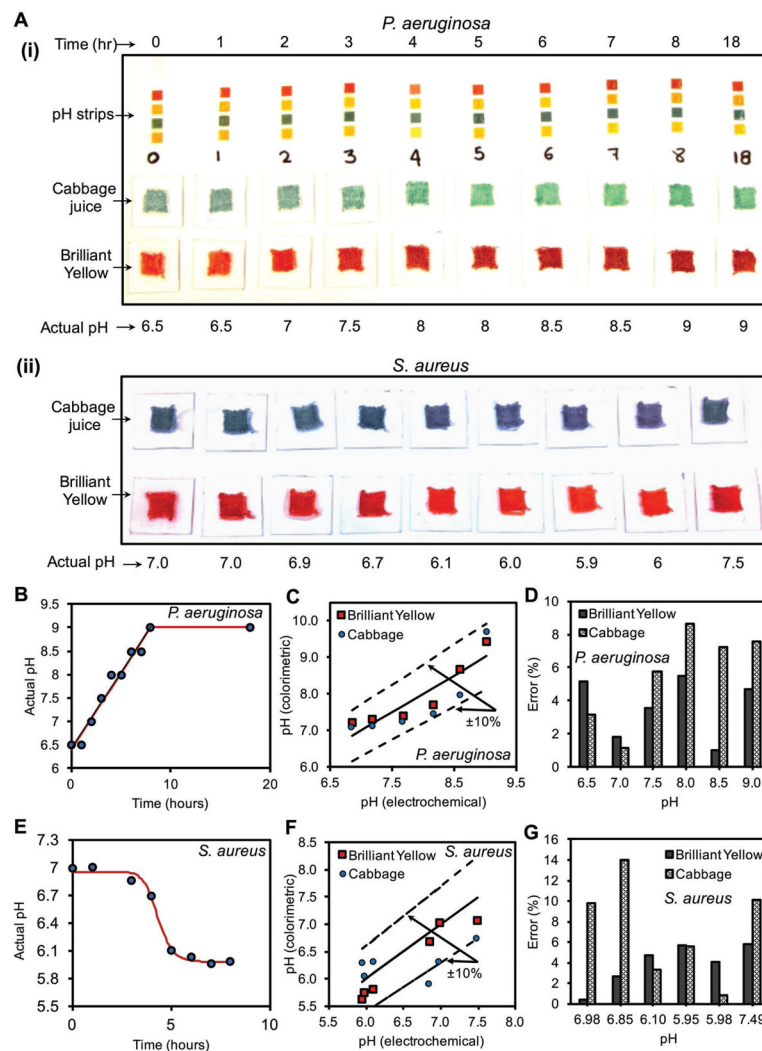
Figure 4.
Colorimetric detection of pH changes due to bacterial growth using GelDerm. A-i,ii) Measurement of pH variations with culture time for *P. aeruginosa* and *S. aureus* using commercial strips, porous sensors. B) pH values measured by a pH probe increased in *P. aeruginosa* cultures over time. C) Measured pH values by the porous sensors as compared to the electrochemical pH probe for *P. aeruginosa* cultures. D) Errors associated with the colorimetric measurement of pH in *P. aeruginosa* cultures as compared to values measured by a pH probe. E) pH values measured by a pH probe decreased in *S. aureus* cultures over time. F) Measured pH values by the porous sensors as compared to the electrochemical pH probe for *S. aureus* cultures. G) Errors associated with the colorimetric measurement of pH in *S. aureus* cultures as compared to values measured by a pH probe.
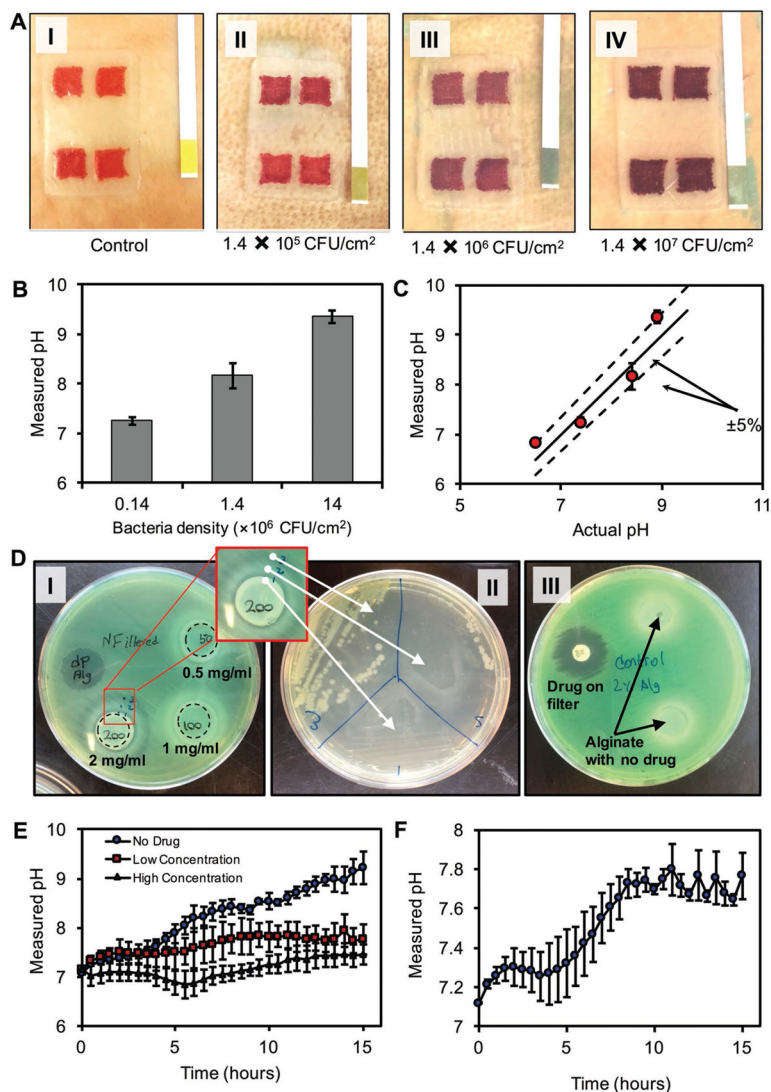
Figure 5.
Ex vivo detection of bacterial infections and evaluation of the antibacterial efficiency of drug-eluting gel using bacteria inhibition assay. A-i–iv) Colorimetric detection of bacterial infection in pig skins. Skins were inoculated at initial densities of 1.4×10^5, 1.4×10^6, and 1.4×10^7 CFU cm^{-2}. After 12 h, GelDerm was placed on samples and images were taken to quantify the pH of the infected skins. B) pH values of infected skins measured by smartphone. C) Comparison of the GelDerm readings with commercially available pH strips. D) Drug-eluting hydrogel disks containing 0.5, 1, and 2 mg mL^{-1} of gentamicin on agar sheets along with a paper disk containing 1 mg mL^{-1} of the same drug as positive control condition. *P. aeruginosa* was cultured on the sheets to observe the effect of the hydrogels on the bacteria. D-i) A clear ring was observable around the 200 mg mL^{-1} hydrogel. D-ii) Samples from three different areas of the ring surrounding the 200 mg mL^{-1} hydrogel were cultured in a different Petri dish to determine whether there is bacterial growth in those areas. D-iii) Hydrogels without any drug content were placed in a separate Petri dish as negative control condition. E) The pH change of pig skin samples inoculated with *P.*

aeruginosa during a 15 h period with three different conditions for drug concentration—0 (no drug), 0.5 mg mL^{-1} (low concentration), and 2 mg mL^{-1} (high concentration). F) The pH change of pig skin samples infected with 1:1 mixture of *P. aeruginosa* and *S. aureus*. Error bars are SD ($n = 3$).
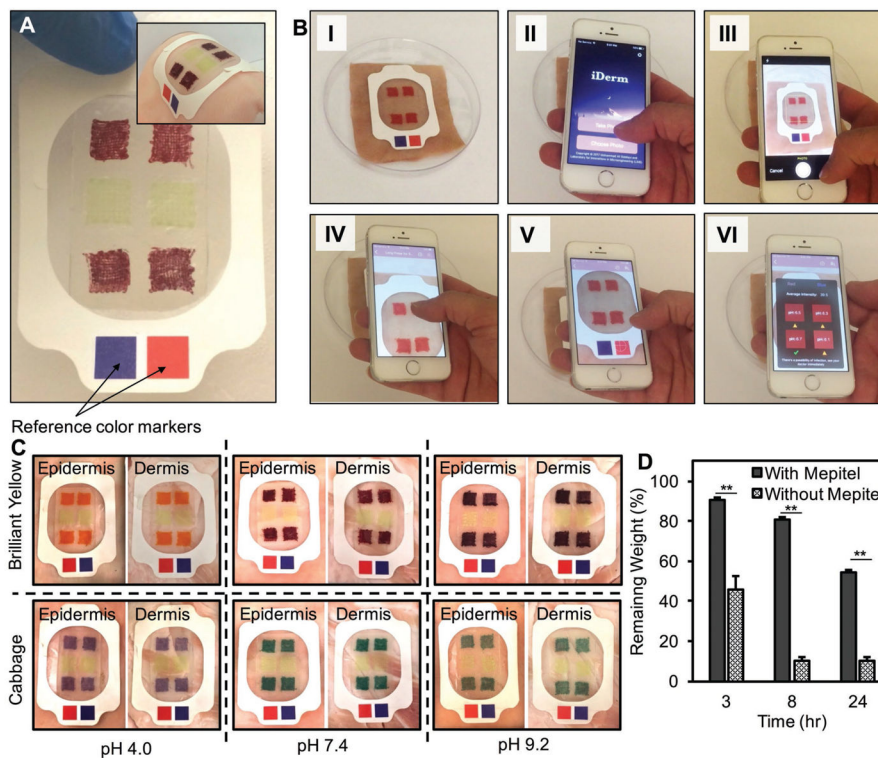
Figure 6.
Integration of GelDerm with commercial dressings. A) GelDerm was integrated with Mepitel; the red and blue squares on the film are reference color markers used for correcting the grayscale intensity and eliminating the effect of lighting condition in the environment on the detected pH. Inset shows GelDerm/Mepitel placed on a piece of pig skin showing good adhesion to the tissue under bending. B) Image sequences demonstrating image capture and processing using iDerm. C) Images of GelDerm/Mepitel dressings placed on the dermis and epidermis layers of pig skin sprayed with different pH values; color change in pH sensors can be correlated to pH change of the skin and can also be observed visually. D) Dehydration of GelDerm/Mepitel as compared to GelDerm alone, showing a significant reduction in the dehydration of GelDerm when it was used with the commercial dressing. Error bars represent the SD ($n = 3$); **$p < 0.005$.